TDA Progress Report 42-118

August 15, 1994

The Long-Term Forecast of Station View Periods

M. W. Lo
Mission Design Section

Using dynamical systems theory, a definite integral is obtained that gives the average view period of a ground station for spacecraft in circular orbits. Minor restrictions exist on the class of circular orbits to which this method can be applied. This method avoids the propagation of the orbit, which requires a lot of resources, and simplifies the algorithm used to compute the mean station view period. The integral is used for long-term station load forecast studies. It also provides a quantitative measure of the effectiveness of a ground station as a function of its latitude.

I. Introduction

Planners for the Deep Space Network frequently need to perform long-term station loading studies to determine resource allocations. Typical questions asked by the planners are as follows:

(1) Will the current 34-m subnet be adequate for the support of mission set A for the next 5 years? The mission set represents a collection of current and planned missions that requires support from the subnet.

(2) How will either adding or removing a station at location X affect the performance of the 26-m subnet for the support of mission set B? Will the performance improve if location Y is selected instead of X?

It is important to make the distinction between short-term planning and long-term planning, because the problems encountered are very different. In this article, problems lasting less than a month are defined as short-term planning problems, or scheduling problems; problems lasting more than a month are defined as long-term planning problems, or forecasting problems. The period of 1 month, while somewhat arbitrarily selected, is a convenient demarcation.

With scheduling problems, the interest is in the actual times of events, such as the start and stop times of the view periods of a particular ground station for a set of spacecraft. Typically, the prediction of orbital ephemeris for scheduling activities must be performed weekly or more often due to the various perturbations that cause the actual orbits to quickly drift away from the predicted orbits. Many of the perturbations have random components, and some of the perturbations are not well understood; these factors make their prediction practically impossible. Thus, scheduling problems are concerned with very short durations not far into the future.

With forecasting problems, the interest is not in the actual times of the events but in their long-term trends and cycles. With such problems, the short-term variations are typically ignored due to

their variability and unpredictability. This is usually achieved by averaging techniques; for example, one finds the mean of a parameter by integration over time. Thus, forecasting problems are concerned with long-term trends and average behavior far into the future.

One way to obtain station loading trends is to compute the station view periods, assuming some perturbation models, and then to compute statistics from this database. This has been the method of choice since it is reasonably straightforward to implement. In order to obtain the station view periods, the satellite ephemeris must be propagated. When the period of analysis is 5 to 10 years for a mission set of dozens of spacecraft, this quickly becomes a data-intensive computational problem. For example, using an analytical orbit generator, to compute the view periods of an Earth-orbiting spacecraft with an altitude around 1000 km for the DSN 26-m subnet for the duration of 1 year requires roughly 20 min on a high-speed workstation. For a more complicated orbit generator, with a larger mission set and a longer duration, say 5 years, the time required to generate the view periods alone would be considerable. Thereafter, the large view-period data set requires additional software for manipulation and computation to produce the desired statistics.

Another way to obtain station loading trends is to consider dynamical systems methods. Dynamical systems is the interdisciplinary field that evolved from the qualitative study of differential equations, first begun by Henri Poincaré at the turn of the century. When one sees the adjective "qualitative," one usually assumes no quantitative results can be obtained from such methods. Fortunately, this is not always the case. But the quantities estimated by qualitative methods tend to be global in nature. This article presents an integral that gives the average view period of a spacecraft to a ground station and is derived using dynamical systems theory.[1]

II. The Long-Term Station View Period Ratio, ρ

An integral was obtained that represents the long-term station view period ratio, ρ, for the class of circular orbits with nonrepeating ground tracks. This ratio provides an estimate of the total time a station is in view of a spacecraft divided by the total elapsed time. More precisely, let

$$T = \text{ total elapsed time}$$

$$P(T) = \text{ total station view period during the elapsed time } T$$

then the long-term station view period ratio is defined by

$$\rho = \lim_{T \to \infty} \frac{P(T)}{T} \tag{1}$$

Thus, given a time period, T, the total amount of time a station is in view of the satellite is given by the following expression:

$$V(T) = \rho T \tag{2}$$

As the ratio, ρ, is a limit, the larger the value of T, the closer $P(T)$ is to $V(T)$. For example, for a 200-km circular orbit with an inclination of 28.5 deg (Case 1, Table 1), the total view period at a ground station at 0-deg latitude for 1 year as computed by $P(T)$ and $V(T)$ is

$$P(1 \text{ year}) = 0.021014 \text{ year}$$

$$V(1 \text{ year}) = 0.021030 \text{ year}$$

[1] An article describing the full derivation of the integral is under preparation.

Here $P(T)$ is computed by propagating the orbit and finding all of the view periods of the station at latitude 0 deg; $V(T)$ is computed from Eq. (2), where the ratio, ρ, is given by the integral.

Preliminary numerical results indicate excellent agreement between the numerical and the theoretical values for the view period ratio, ρ, for circular orbits. The numerical values are computed typically from 1 year's worth of station view periods. For the circular orbits used in the numerical study, $\Delta\rho$ is less than ± 0.2 percent, where $\Delta\rho$ is the difference between the theoretical and numerical values of ρ. For the elliptic orbits used in the numerical study, at $e = 0.05$, the maximum $\Delta\rho$ for the cases tested exceeds 15 percent. For orbits whose period is commensurate with the Earth's rotational period, the $\Delta\rho$ for the cases tested is within ± 1.5 percent. These results are tabulated in Tables 1 through 3 and discussed in Section V.

III. Heuristics and Theoretical Background

Examine first the geometry of the spacecraft and the ground station. Figure 1 shows the geometry of the station mask, which is determined by the altitude of the spacecraft and has the following interpretation. The station mask is the circle of angular radius, θ_0, about the ground station. When the spacecraft ground track is within the station mask, the spacecraft is in view of the station. When the ground track is outside of the station mask, the spacecraft is not in view of the station. The angle, ε, is the minimum station elevation angle below which the station cannot view the spacecraft, due to some constraint or obstruction at the horizon. In particular, when the spacecraft-to-station elevation angle is ≤ 0 deg, then the Earth itself is obstructing the spacecraft from the station view. A spherical Earth is assumed here.

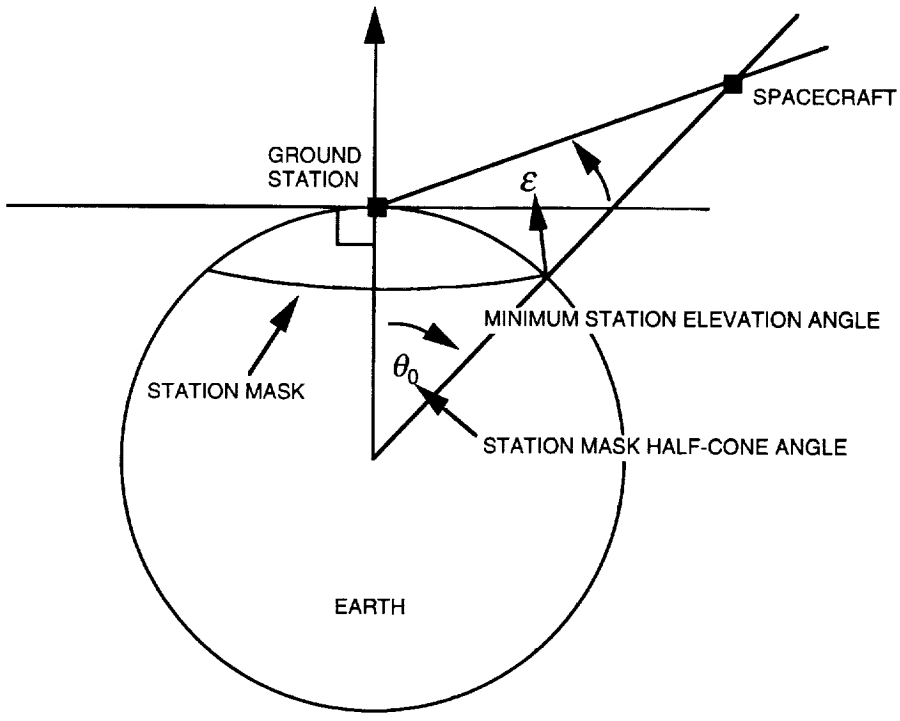

Fig. 1. Geometry of the station mask.

Figure 2 illustrates the ground tracks of a spacecraft in circular orbit at a 7714.14-km radius (this is the radius of the TOPEX/POSEIDON orbit) and a 28.5-deg inclination. The circle centered at the equator with the label "Case 4" is the station mask of a fictitious station on an ocean platform at the equator (latitude = 0 deg) with longitude equal to that of the 26-m station at Goldstone. The station

mask of the Madrid station is labeled "Case 7" and that of the Canberra station is labeled "Case 6." They are only partially in view. Consider a station at the pole; its mask is the cap about the pole. For the spacecraft in Case 4, this cap does not intersect the ground track pattern. This means that the spacecraft would not see the station at the pole. The Madrid station mask (Case 7) intersects the ground tracks in a much smaller area than that of Case 4. Intuitively, one might think that, somehow, the total view period (sum of all the view periods) is proportional to the area of the intersection between the band of the ground track and the station mask. After all, when there is no intersection, there is no view period. When there is a lot of intersection, there is a large view period. But, unfortunately, this is not the whole story. There are other factors.

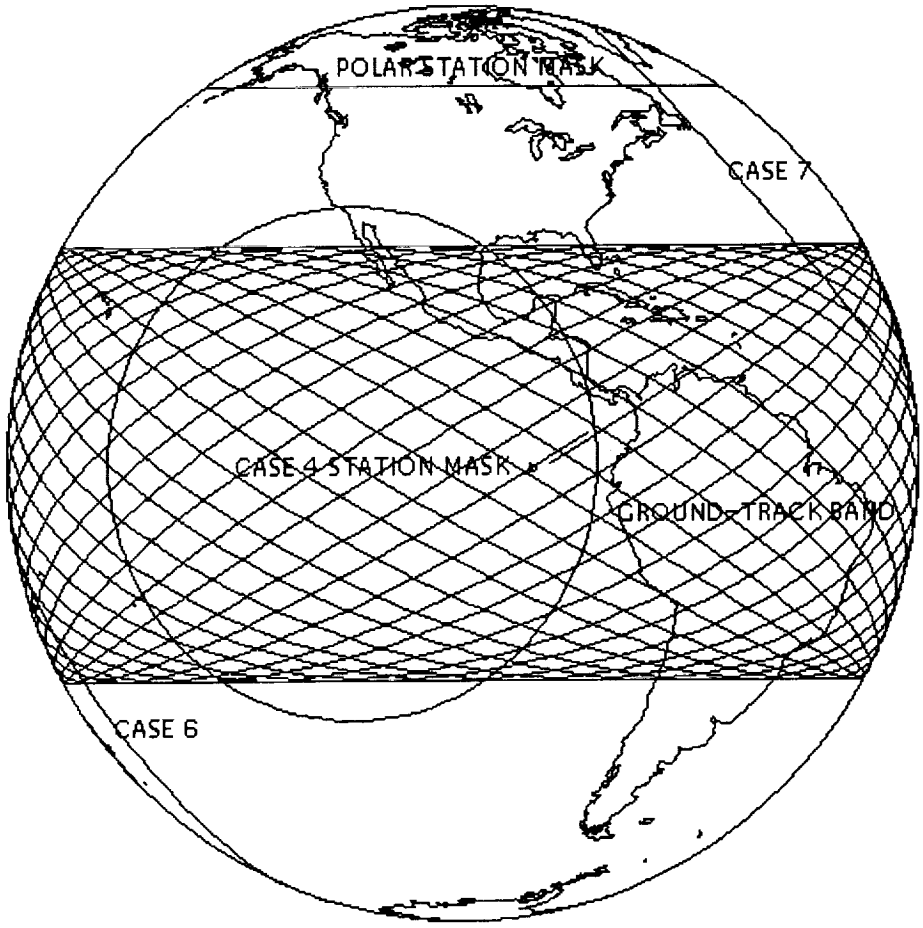

Fig. 2. Station masks and ground tracks for cases 4, 6, and 7 (orthographic projection).

Consider the following example: suppose now that the orbit is of sufficiently high inclination and low altitude that the station mask is a small circle completely within the ground track band, as illustrated in Fig. 3. Calculations quickly show that Station 1 has a much higher total view period than Station 2, even though they have the same mask area and are both enveloped by the spacecraft ground tracks. This agrees with the well-known observation that stations at higher latitudes tend to have more and longer view periods.

This problem is resolved by looking at Fig. 2 more carefully. Notice that the ground tracks are more closely packed near the top than near the equator. Furthermore, the speed of the spacecraft nadir along the ground track is not constant even though that of the circular orbit is constant. This is due to the

rotation of the Earth and the projection of the spacecraft motion onto the sphere. Thus, the time spent near the equator and that near the top and bottom of the ground track band is not the same. However, the station mask is unaffected by the rotation of the Earth, and it has the same size regardless of the location of the station. Hence, going back to Fig. 3, even though the two station masks contain the same amount of ground track area, the actual time spent in each area is not the same. Thus, one has to use a weight factor to compute the area of intersection in order for it to be proportional to the total view period. In mathematical terms, one needs to find an invariant measure for the dynamics. This measure will give the connection between the weighted area of the mask and the time spent in the mask. This has been done for the case of circular orbits with certain mild restrictions and is discussed in the next section.

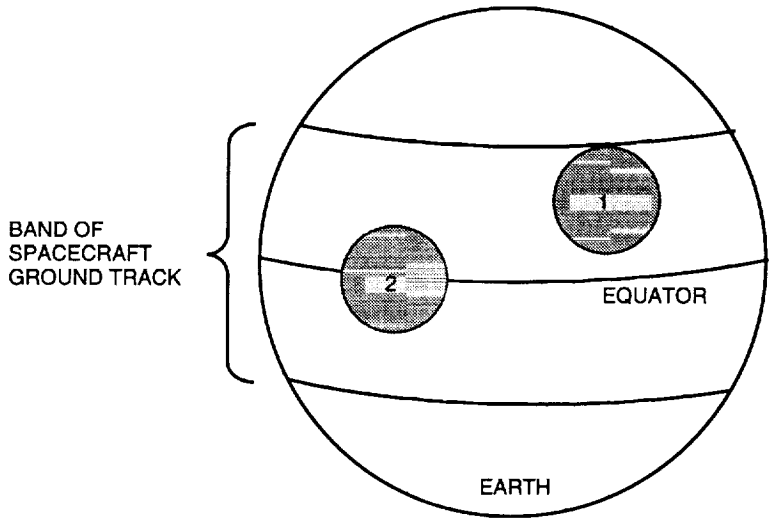

Fig. 3. Station masks at different latitudes.

The system of spacecraft ground tracks belongs to a class of dynamical systems known as "ergodic." The discussion on ergodic theory below drew on [1–3]. The analysis used many of the ideas described in [4]. The important property about ergodic systems for this discussion is the following.

Let $F(x)$ be a well-behaved function on the space where there is an ergodic system. Then the time mean of F and the space mean of F are equal. The time mean of F is the path integral of $F(x)$ along the trajectory as a function of time. The space mean of F is simply the integral of F over the space. This is known as the Ergodic Theorem.

Now let F be the station view function. This means F is equal to 1 when the spacecraft is in view of the station, and F is equal to 0 otherwise. The time mean of F is just the time average of the total view period. The view periods require a lot of calculations, which one would like to avoid. But the Ergodic Theorem states that one can skip all this computation by simply calculating the space mean of F. This is a great simplification; notice that the space mean of F is just its integral over the sphere, which is easy to compute. One arrives at the following:

$$\lim_{T\to\infty} \frac{P(T)}{T} = \text{time mean of } F$$

$$\int_{EARTH} F(x)d\mu = \text{space mean of } F$$

$$\rho = \lim_{T\to\infty} \frac{P(T)}{T} = \int_{EARTH} F(x)d\mu$$

The construction of the weight function, μ, also known as the invariant measure, is geometric in nature. Referring back to Fig. 2, follow a small segment along the ground tracks and see how it gets stretched as time progresses. This stretching factor then enables one to compute μ. It is this weight function that enables one to relate the time with the area. Having done so, it becomes an easy task to perform the integral, F, whereupon, one has computed the long-term view period ratio, ρ. This demonstrates the power of qualitative methods even for engineering applications.

IV. The Integral Representation of ρ

The integral ρ for a spacecraft in circular orbit is subject to the following perturbations and constraints:

(1) The spacecraft is in circular orbit; the orbit eccentricity is 0.

(2) The spacecraft is perturbed only by the linear J_2 term of the spherical harmonic expansion of the gravity field of Earth. Thus, the first-order linear perturbations for the node and argument of perigee are:

$$\Omega(T) = \Omega_0 + \frac{d\Omega}{dt} T$$

$$\omega(T) = \omega_0 + \frac{d\omega}{dt} T$$

The derivatives $d\Omega/dt$ and $d\omega/dt$ are constant. The semimajor axis, eccentricity, and inclination are constant. Mean elements are assumed throughout this discussion.

(3) The orbit inclination is not 0 deg. Circular orbits with a 0-deg inclination have constant view periods that can be easily calculated.[2]

(4) The orbit has an orbital period that is incommensurate with the period of the Earth's rotation. Hence, this orbit does not have repeating ground tracks.

(5) The ground station is not centered at the north or south pole.

(6) The intersection of the station mask with the ground-track region forms a simply connected domain.

The variables and the integral for ρ are

$$\left.\begin{aligned} \rho &= \text{long} - \text{term station view period ratio} \\ \varphi_0 &= \text{station latitude} \neq \pm 90 \text{ deg} \\ \theta_0 &= \text{station mask angular radius} \\ &= \arccos\,(R_E/R) \text{ for stations with } \varepsilon = 0 \text{ deg} \\ R_E &= \text{Earth radius} \\ R &= \text{spacecraft orbit radius} \\ \varepsilon &= \text{minimum station elevation angle} \end{aligned}\right\} \quad (3a)$$

[2] M. W. Lo, "The View Period of Circular Equatorial Orbits," JPL Interoffice Memorandum 312/94.7-10 (internal document), Jet Propulsion Laboratory, Pasadena, California, June 3, 1994.

$$
\left.
\begin{aligned}
i &= \text{spacecraft orbit inclination } > 0 \text{ deg} \\
L_i &= \begin{cases} i \text{ if } i \leq 90 \text{ deg} \\ 180 - i \text{ if } i > 90 \text{ deg} \end{cases} \\
\varphi_1 &= \max\{\varphi_0 - \theta_0, -L_i\} \\
\varphi_2 &= \min\{\varphi_0 + \theta_0, L_i\} \\
f(\varphi) &= \frac{\cos\varphi \arccos\left(\frac{\cos\theta_0 - \sin\varphi \sin\varphi_0}{\cos\varphi_0 \cos\varphi}\right)}{\pi^2\sqrt{(\sin^2 i - \sin^2\varphi)}} \\
\rho &= \int_{\varphi_1}^{\varphi_2} f(\varphi)d\varphi
\end{aligned}
\right\} \tag{3b}
$$

V. Numerical Verification

Three sets of tests were performed to verify the algorithm. The first set used circular orbits; the results are shown in Table 1. The second set used elliptic orbits with eccentricity = 0.05; the results are shown in Table 2. The third set used orbits with repeating ground tracks; the results are shown in Table 3. The parameter that measures the accuracy of the model is $\Delta\rho$ (listed in the last column of the tables):

$$\Delta\rho\% = 100\,\frac{\rho_{\text{THEORY}} - \rho_{\text{NUMERIC}}}{\rho_{\text{NUMERIC}}}$$

Table 1 lists the 31 cases used in the verification of Eq. (3). The numerical view periods are generated by propagating the orbit using the linear J_2 perturbations. The integral for ρ is evaluated using a mathematical symbolic computation program. The low Earth orbits selected for the verification have various altitudes with inclinations at 28.5, 48, 88.5, 98.5, and 151.5 deg. For those cases with an asterisk in front of the inclination, the orbit propagation begins at the descending node. For all other cases, the orbit propagation begins at the ascending node. The cases in Table 3 use an orbit with repeating ground tracks with a repeat pattern of 20 orbits in 3 days. All other orbits have nonrepeating ground tracks; thus, their periods are incommensurate with that of the period of the Earth's rotation.

The stations at latitudes of 0, 5, and 10 deg have the longitude of the 24-m Goldstone DSN station. The stations at latitudes of −35.4 and 40.4 deg are the 24-m Canberra and Madrid DSN stations, respectively.

The $\Delta\rho$ for the circular orbits of Table 1 are plotted in Fig. 4. It shows the differences between the theoretical and numerical values of ρ for these orbits to be under 0.2 percent, indicating excellent agreement.

Figure 5 plots the $\Delta\rho$ of the circular orbits from Table 1 as a solid curve on top of which the values for the corresponding elliptic orbits from Table 2 have been added. For example, Case E1 and Case 4 in Fig. 5 have the same test parameters except for the orbit eccentricity. By changing the eccentricity of the orbit of Case 4 to 0.05 while keeping all other parameters fixed, $\Delta\rho$ increased from under 0.2 percent to about 1 percent. But for Case 23, the change in eccentricity and the high inclination caused $\Delta\rho$ to exceed 15 percent. This shows that the algorithm does not work as well for elliptic orbits. However, the accuracy may be sufficient for load studies since many of the parameters are even less well known.

Figure 6 plots the $\Delta\rho$ of orbits with repeating ground tracks from Table 3; a single fixed orbit with a repeat pattern of 20 orbits in 3 days is used with different stations for these cases. The difference between the theoretical and numerical values of ρ is still quite good at less than 1.3 percent.

Table 1. Comparison of numerical versus theoretical long-term view period ratio for circular orbits with nonrepeating ground tracks (eccentricity = 0).

Case number[a]	Orbit radius, km	Orbit inclination,[b] deg	Station latitude[c]	Numeric[d]	Theory[e]	Difference[f]	Percentage[g]
1	6578.14	28.5	0.0	0.021014	0.021030	0.000015	0.072847
2	6578.14	28.5	−35.4	0.014719	0.014740	0.000020	0.138198
3	6578.14	28.5	40.4	0.004976	0.004985	0.000009	0.178944
4	7714.14	28.5	0.0	0.154513	0.154505	−0.000008	−0.005178
5	7714.14	28.5	5.0	0.148701	0.148664	−0.000037	−0.024882
6	7714.14	28.5	−35.4	0.085387	0.085383	−0.000004	−0.004685
7	7714.14	28.5	40.4	0.073382	0.073393	0.000011	0.014854
8	7714.14	*28.5	0.0	0.154513	0.154505	−0.000008	−0.005178
9	7714.14	*28.5	−35.4	0.085368	0.085383	0.000015	0.017454
10	7714.14	*151.5	0.0	0.154543	0.154505	−0.000038	−0.024589
11	7714.14	*151.5	−35.4	0.085507	0.085383	−0.000124	−0.145017
12	7714.14	*151.5	40.4	0.073483	0.073393	−0.00009	−0.122614
13	7714.14	151.5	5.0	0.148658	0.148664	0.000006	0.004036
14	7714.14	151.5	−35.4	0.085361	0.085383	0.000022	0.025421
15	7714.14	151.5	40.4	0.073422	0.073393	−0.000029	−0.039498
16	7714.14	48.0	0.0	0.081425	0.081432	0.000007	0.008351
17	7714.14	48.0	5.0	0.082509	0.082453	−0.000056	−0.067993
18	7714.14	48.0	10.0	0.086041	0.086012	−0.000029	−0.033821
19	7714.14	48.0	−35.4	0.100203	0.100189	−0.000014	−0.013972
20	7714.14	48.0	40.4	0.096789	0.0968	0.000011	0.011675
21	7714.14	61.0	0.0	0.067089	0.067078	−0.000011	−0.016424
22	7714.14	61.0	−35.4	0.099756	0.099737	−0.000019	−0.018588
23	7714.14	61.0	40.4	0.102233	0.102237	0.000004	0.003912
24	7714.14	88.5	0.0	0.057763	0.057726	−0.000037	−0.064401
25	7714.14	88.5	−35.4	0.072831	0.07285	0.000019	0.025538
26	7714.14	88.5	40.4	0.079102	0.079127	0.000025	0.031731
27	7714.14	98.5	0.0	0.05849	0.058413	−0.000077	−0.132331
28	7714.14	98.5	−35.4	0.074554	0.074609	0.000055	0.073638
29	7714.14	98.5	40.4	0.081762	0.081743	−0.000019	−0.02385
30	10,000.14	61.0	0.0	0.15332	0.153309	−0.000011	−0.007175
31	10,000.14	61.0	5.0	0.155375	0.155142	−0.000233	−0.14996

[a] Circular orbits. All orbits have nonrepeating ground tracks.
[b] The * indicates the orbit propagation started at the descending node. All other cases started at the ascending node.
[c] The stations with latitudes at 0, 5, and 10 deg have the longitude of the Goldstone station. The station with latitude at −35.4 deg is the Canberra station. The station with latitude at 40.4 deg is the Madrid station.
[d] (Total view periods)/(total time), numerically generated using linear J_2 orbit propagation.
[e] Limit (total view periods)/(total time), theoretical value.
[f] Theory − numeric.
[g] (Difference/numeric) × 100.

Table 2. Comparison of numerical versus theoretical long-term view period ratio for elliptical orbits (eccentricity = 0.05).

Case number[a]	Orbit radius, km	Orbit inclination,[b] deg	Station latitude[c]	Numeric[d]	Theory[e]	Difference[f]	Percentage[g]
E1	7714.14	28.5	0.0	0.152476	0.154505	0.002029	1.33082
E2	7714.14	28.5	−35.4	0.086059	0.085383	−0.000676	−0.785138
E3	7714.14	28.5	40.4	0.072582	0.073393	0.000811	1.11773
E4	7714.14	61.0	0.0	0.067196	0.067078	−0.000117	−0.174601
E5	7714.14	61.0	−35.4	0.112791	0.099737	−0.013054	−11.5733
E6	7714.14	61.0	40.4	0.088053	0.102237	0.014184	16.1085
E7	7714.14	88.5	0.0	0.057875	0.057726	−0.000149	−0.256726
E8	7714.14	88.5	−35.4	0.071308	0.072850	0.001542	2.16308
E9	7714.14	88.5	40.4	0.081627	0.079127	−0.002500	−3.0623
E10	10,000.14	28.5	0.0	0.261715	0.261864	0.000149	0.056955
E11	10,000.14	28.5	−35.4	0.173428	0.173361	−0.000067	−0.038629
E12	10,000.14	28.5	40.4	0.158665	0.158644	−0.000021	−0.012950
E13	10,000.14	61.0	0.0	0.153501	0.153308	−0.000193	−0.125588
E14	10,000.14	61.0	−35.4	0.19271	0.18373	−0.008980	−4.65991
E15	10,000.14	61.0	40.4	0.17489	0.184627	0.009736	5.56719

[a] Elliptical orbits. All orbits have nonrepeating ground tracks.
[b] All cases started at the ascending node.
[c] The stations with latitudes at 0, 5, and 10 deg have the longitude of the Goldstone station. The station with latitude at −35.4 deg is the Canberra station. The station with latitude at 40.4 deg is the Madrid station.
[d] (Total view periods)/(total time), numerically generated using linear J_2 orbit propagation.
[e] Limit (total view periods)/(total time), theoretical value.
[f] Theory − numeric.
[g] (Difference/numeric) x 100.

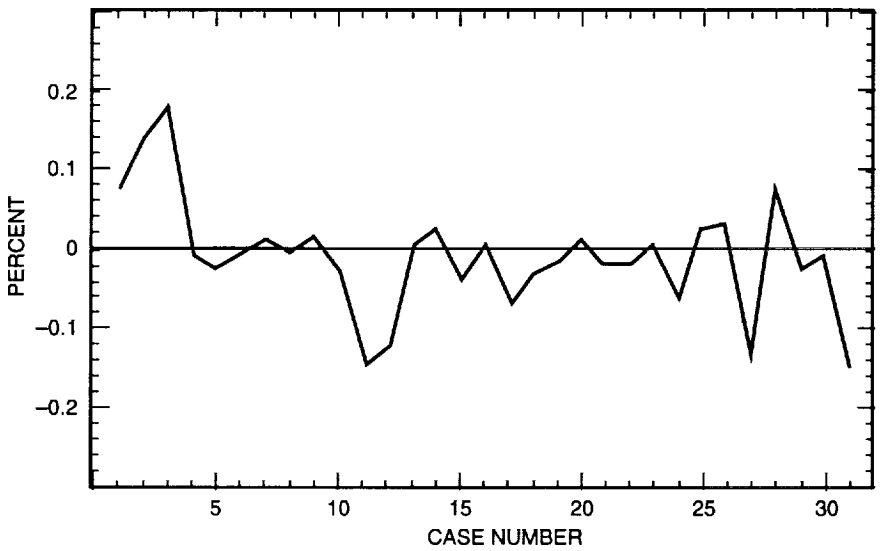

Fig. 4. Difference of theoretical versus numerical long-term view period ratio (all orbits with eccentricity = 0, see Table 1).

Table 3. Comparison of numerical versus theoretical long-term view period ratio for circular orbits with repeating ground tracks (eccentricity = 0).

Case number[a]	Orbit radius, km	Orbit inclination,[b] deg	Station latitude[c]	Numeric[d]	Theory[e]	Difference[f]	Percentage[g]
P1	11889.43	28.5	0.0	0.306147	0.30619	0.000043	0.014046
P2	11889.43	28.5	5.0	0.305175	0.305147	−0.000028	−0.009175
P3	11889.43	28.5	10.0	0.301975	0.301929	−0.000046	−0.015233
P4	11889.43	28.5	28.5	0.258294	0.258513	0.000219	0.084787
P5	11889.43	28.5	−35.4	0.226208	0.224439	−0.001769	−0.782024
P6	11889.43	28.5	−35.4	0.22622	0.224439	−0.001781	−0.787287
P7	11889.43	28.5	40.4	0.204349	0.206974	0.002625	1.284567
P8	11889.43	28.5	40.4	0.204369	0.206974	0.002605	1.274655

[a] Circular orbits with a (3/20) repeat pattern (20 orbits in 3 days).
[b] All cases started at the ascending node.
[c] The stations with latitudes at 0, 5, and 10 deg have the longitude of the Goldstone station. The station with latitude at −35.4 deg is the Canberra station. The station with latitude at 40.4 deg is the Madrid station.
[d] (Total view periods)/(total time), numerically generated using linear J_2 orbit propagation.
[e] Limit (total view periods)/(total time), theoretical value.
[f] Theory − numeric.
[g] (Difference/numeric) x 100.

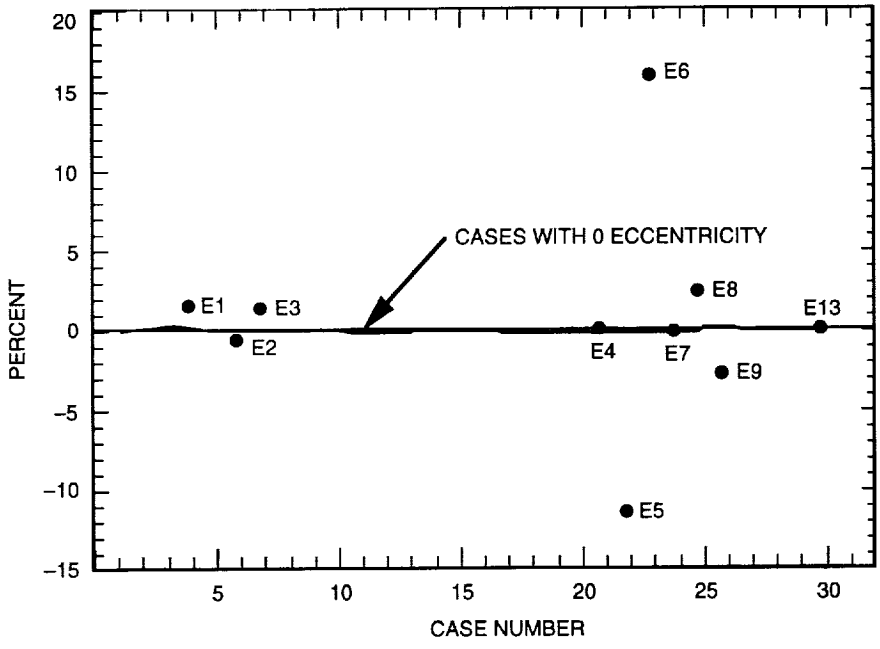

Fig. 5. Comparison of circular and elliptical orbits: difference of theoretical versus numerical long-term view period ratio (see Table 2).

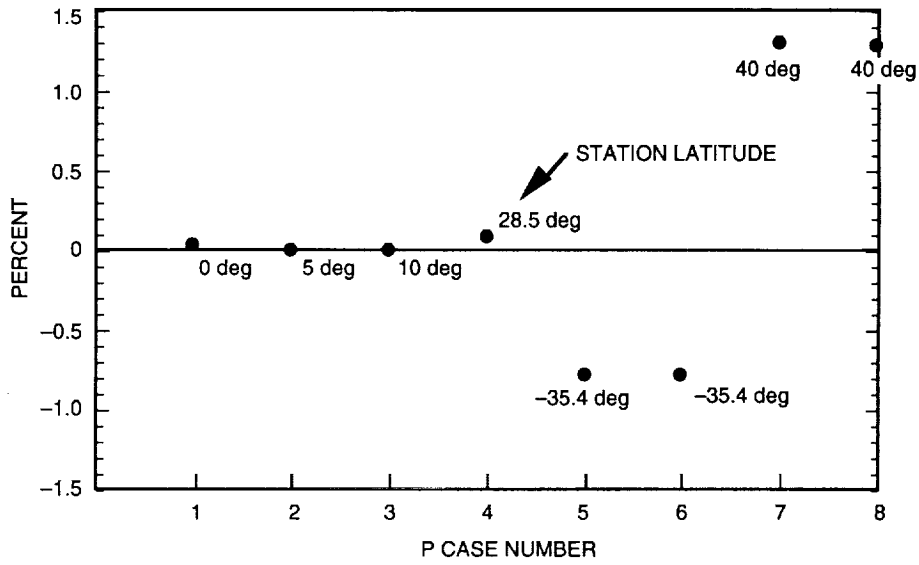

Fig. 6. Difference of theoretical versus numerical long-term view period ratio for orbits with repeating ground tracks (see Table 3).

These results indicate that putting the circular orbit at different inclinations, altitudes, and nodes does not greatly affect the agreement between the numerical and theoretical values for the view period ratio, ρ. The errors are all within 0.15 percent. The error goes up by a factor of 10 when the orbit ground tracks are repeating, but a fairly good agreement is retained.

VI. Applications

The definite integral for ρ is easily integrated using a mathematical symbolic computation program, each case requiring seconds. As mentioned before,

$$\rho T = \text{total view periods during elapsed time } T$$

is a good estimate of the total station view period. Thus,

$$\rho \text{ 24 hr} = \text{average daily total view periods}$$

$$\rho \text{ 7 days} = \text{average weekly total view periods}$$

and so on are some useful numbers that are very easy to compute.

Now consider a more interesting problem. Suppose one has a spacecraft and K ground stations. Compute ρ for each station: $\rho_1, \rho_2, \cdots, \rho_K$. Suppose the spacecraft requires τ sec daily for downlink using these stations. The following sum represents the maximum average contact time possible with the K ground stations:

$$C = (\rho_1 + \rho_2 + \cdots + \rho_K) \text{ 24 hr}$$

If $\tau > C$, then it means there is not enough contact time on the average for the spacecraft to downlink its data. But if $\tau < C$, one cannot say very much since the overlaps between the ground stations are not known. However, if, for example, $\tau/C < 0.5$, then it seems very likely the ground stations will be able to satisfy the downlink requirement. One can look at the geometry of the overlap of the station masks to further refine this approximation.

This approach gives a very quick way to bound performance. One can consider other scenarios of N spacecraft with K stations and so on. This would be a good capability to place into a spreadsheet program to provide quick estimates for what-if studies. It also has the advantage that the theoretical basis of the method is well understood so that one need not have that uncomfortable feeling that frequently accompanies statistical analyses not as well understood.

Another application is the performance measure for the location of ground stations. The definite integral, ρ, provides a quantitative measure of the well-known observation that ground stations at higher latitudes generally have more and longer view periods.

These applications require further refinement but indicate the type of calculations possible with this approach.

VII. Discussion

The circularity of the orbits is not as severe a restriction in applications since, according to Negron et al. [5], roughly 75 percent of the Earth spacecraft orbits have eccentricity < 0.05. The sensitivity of the integral in Eq. (3) to eccentricity needs to be determined to see if it can be applied to orbits with lower (but nonzero) eccentricity. With elliptic orbits, the motion of the argument of perigee causes the geometry to change with time, which complicates the situation considerably. The extension of the theory to elliptic orbits is under study. The basic approach may be used, but the problem is more difficult and additional analysis is required to construct the function $F(x)$ and the measure μ.

The period noncommensurability requirement appears to be restrictive, since orbits with repeating ground tracks are very useful and popular. However, as Cases 26 to 33 show, the same integral provides a fairly good estimate of ρ to within 1.3 percent. In fact, for stations at low latitudes, the estimate is good to within 0.015 percent. This seemed surprising at first; but when one considers the fact that any orbit can be approximated by one with repeating ground tracks to an arbitrary degree of precision, it seems less surprising. Also, the number of different view periods of orbits with repeating ground tracks is finite and can easily be determined numerically. Of course, for orbits that are geosynchronous, this integral does not make sense at all. But the view periods for such orbits are trivial. Additional analysis is required to determine the limits of applicability of the integral to orbits with periodic ground tracks.

The integral for ρ, Eq. (3), depends on the following parameters only: $\{R_E, R, i, \phi_0\}$, which are the Earth radius, spacecraft orbit radius and inclination, and the station latitude. The station longitude, the orbit node, and J_2 do not appear in the equation. Since this is an averaging process, the absence of the station longitude and orbit node is reasonable. These two parameters should simply average out in the long term. The absence of J_2 is surprising. But, it is actually hidden in the requirement that the orbit period be incommensurate with that of the rotation period of the Earth. And it is not so surprising in light of the Ergodic Theorem, which states that the details of the dynamics such as rates and the equations of motion that appear on the time-mean side of Eq. (3) can be replaced with an area integral on the space-mean side of Eq. (3). Thus, J_2 and other dynamic quantities appear only in the time mean but not in the space mean.

The tests described in Table 1 and in Section V above indicate an excellent agreement between the numerically computed values for ρ and those computed from Eq. (3). However, additional numerical results are also needed to further substantiate the theoretical results and scope the limits of applicability.

Work continues on this approach to analyze station load forecasts. The extension of the integral to elliptic orbits is highly desirable. Other dynamical systems methods can be used to refine the forecasts, giving statistical data of more resolution than the mean. These are also being explored.

Acknowledgments

The author would like to thank Johnny H. Kwok and Steven Matousek of JPL for bringing this problem to his attention; Lawrence E. Bright, Jeff A. Estefan, David L. Farless, Johnny H. Kwok, and Mark A. Vincent of JPL for the invaluable input and review of this article; and Professors H. B. Keller and S. Wiggins of the California Institute of Technology for several useful discussions. The author would also like to thank Charles D. Edwards and Vincent Pollmeir for their support. In particular, the author would like to thank Warren L. Martin of JPL for his strong support, which made this work possible.

References

[1] V. I. Arnold, *Ergodic Problems of Classical Mechanics*, New York: Addison-Wesley, 1989.

[2] I. E. Farquhar, *Ergodic Theory in Statistical Mechanics*, New York: John Wiley & Sons, 1964.

[3] K. Petersen, *Ergodic Theory*, Cambridge, England: Cambridge University Press, 1983.

[4] V. I. Arnold, *Geometrical Methods in the Theory of Ordinary Differential Equations*, New York: Springer-Verlag, 1983.

[5] D. Negron, Jr., S. Alfano, and D. Wright III, "The Method of Ratios," *Journal of the Astronautical Sciences*, vol. 40, no. 2, pp. 297–309, April–June 1992.